POSSIBLE ION TRAPPING IN RECYCLER RING

K.Y. Ng,* FNAL, Batavia, IL 60510, USA

Abstract

Transverse instabilities have been observed[1] in the antiproton beam stored in the Fermilab Recycler Ring, resulting in a sudden increase in the transverse emittances and a small beam loss. The instabilities appear to occur a few hours after a change in the ramping pattern of the Main Injector which shares the same tunnel. The phenomena have been studied by inducing similar instabilities. However, the mechanism is still unknown. A possible explanation is that the ions trapped in the beam reach such an intensity that collective coupled transverse oscillation occurs. However, there is no direct evidence of the trapped ions at this moment.

I. INTRODUCTION

The Fermilab Recycler Ring is a ring to store, accumulate and stochastically cool antiprotons. Recently, transverse instabilities have been reported in the antiproton beam with the signature of a sudden increase in the transverse emittances and a small loss in beam intensity. The mechanism of the instability is still unknown. However, it has been suggested that these instabilities are related to ions trapped inside the antiproton beam, although no direct verification has been made. An important reason for this suggestion comes from the fact that such transverse instabilities have never been observed when protons are stored.

In this note, we are going to report the instabilities and the various experiments hoping to reveal the mechanism of the instabilities. Finally some possible mechanism is suggested.

The Recycler Ring is a ring with permanent gradient magnets and quadrupoles. Some of its properties are listed in Table 1.

Table 1: Some relevant properties of the Fermilab Recycler Ring.

Circumference (m)	~ 3319.4
Kinetic energy (GeV)	~ 8.00
Revolution frequency (kHz)	89.812
Revolution period (μs)	11.134
Horizontal betatron tune	25.425
Vertical betatron tune	24.415

* Email: ng@fnal.gov. Work supported by the U.S. Department of Energy under contract No. DE-AC02-76CH03000.

[1] All the experimental data reported in this article were gathered by members of the Fermilab Recycler Ring Department. The author of this article just serves as a reporter.

II. INSTABILITIES

Observation

The first such documented transverse instability was observed on February 19, 2004. An antiproton beam of intensity 126×10^{10} and length 7.3 μs was stored in the Recycler Ring between two barrier waves. The horizontal and vertical 95% normalized emittances were cooled stochastically to about 7π mm-mr. The horizontal and vertical emittances were roughly the same because the residual horizontal and vertical betatron tunes were close resulting in strong horizontal and vertical coupling. As seen in the upper plot of Fig. 1, the emittances took a sudden jump to about 15π mm-mr at about 12:00 noon. At the same time, as shown in the lower plot of Fig. 1, there was a small beam

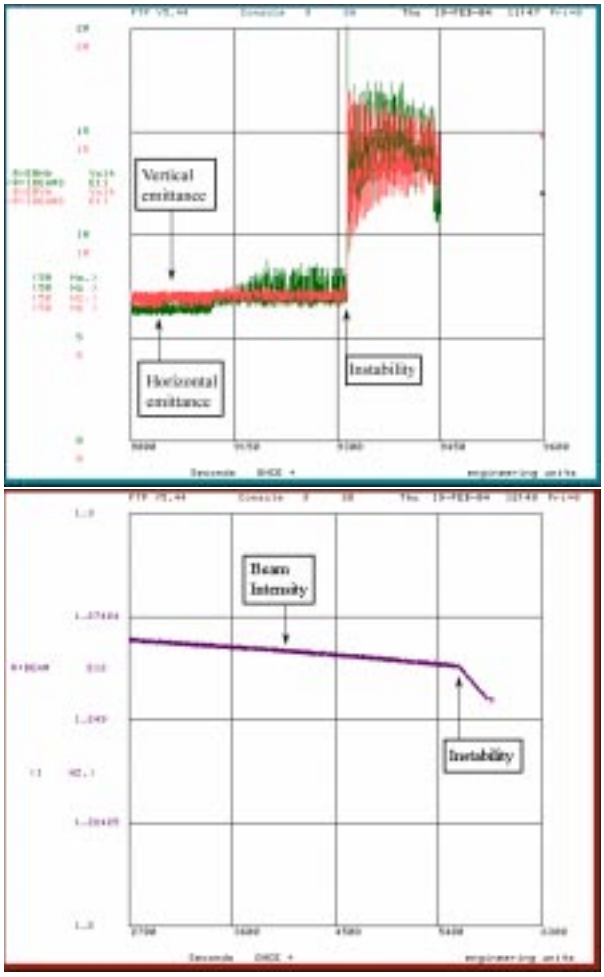

Figure 1: An antiproton beam of intensity 126×10^{10} and length 7.3 μs was seen on February 19 to suffer a transverse instability with a sudden emittance growth and a slight beam loss.

loss of about 1×10^{10}. When the record of the Main Injector, which shares the same tunnel with the Recycler Ring, was traced, it was found that the Main Injector changed its ramp rate a few hours earlier.

Similar instability was next observed on March 8, 2004. This time, a weak antiproton beam of intensity 30×10^{10} and length 9.3 μs confined by two barrier waves was cooled to the horizontal and vertical 95% normalized emittances of about 2.5π mm-mr. As shown in Fig. 2, the emittances jumped to about 7.5π mm-mr at about 2:30 am with a beam loss of 1.0×10^{10}. As shown in the figure, the instability occurred shortly after an I:MAGPWR decrease, which was a decrease in the ramp rate of the Main Injector.

Another instability occurred on April 27 at 1:30 am as shown in Fig. 3. The antiproton beam was initially 125×10^{10} in intensity. In the evening of April 26, the beam

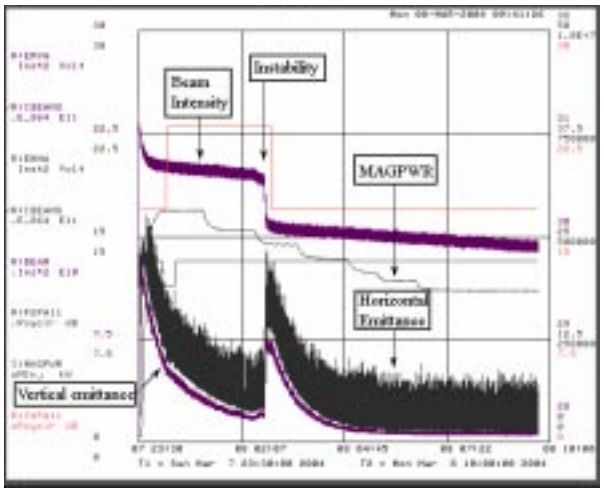

Figure 2: An antiproton beam of intensity 30×10^{10} and length 9.3 μs was seen on March 8 to suffer a transverse instability with a sudden emittance growth and a beam loss of about 20%.

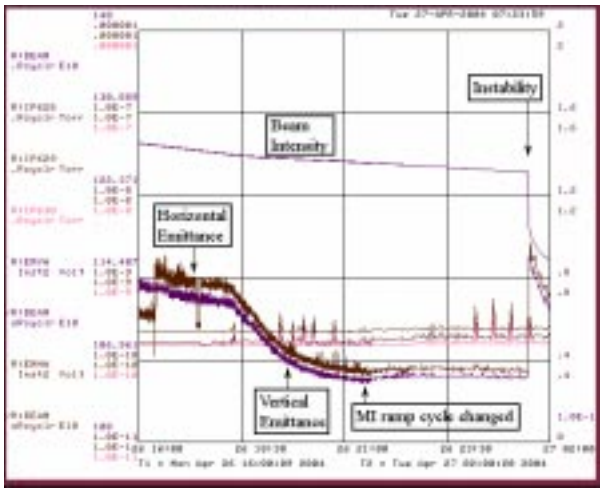

Figure 3: An antiproton beam of intensity 125×10^{10} and length 5.28 μs was seen on April 27 to suffer a transverse instability with a sudden emittance growth and a beam loss of 3.8×10^{10}.

was cooled both transversely and longitudinally. At 21:47, the beam was compressed longitudinally by about 1 μs to 5.28 μs. The rms momentum spread was 3.4 MeV/c and the longitudinal emittance 61.8 eVs. At about this moment, there was a ramping change of the Main Injector. Longitudinal cooling continued with rms momentum spread and longitudinal emittance reduced to 3.0 MeV/s and 54 eVs at 00:10 April 27. At 1:30, the sudden increase in transverse emittances occurred with a small beam loss of 3.8×10^{10}. In Fig. 4, we show the betatron sidebands recorded by the 1.75 GHz Schottky detector before and after the instability. The sidebands shown in the two left and two right small plots had been broadened after the instability.

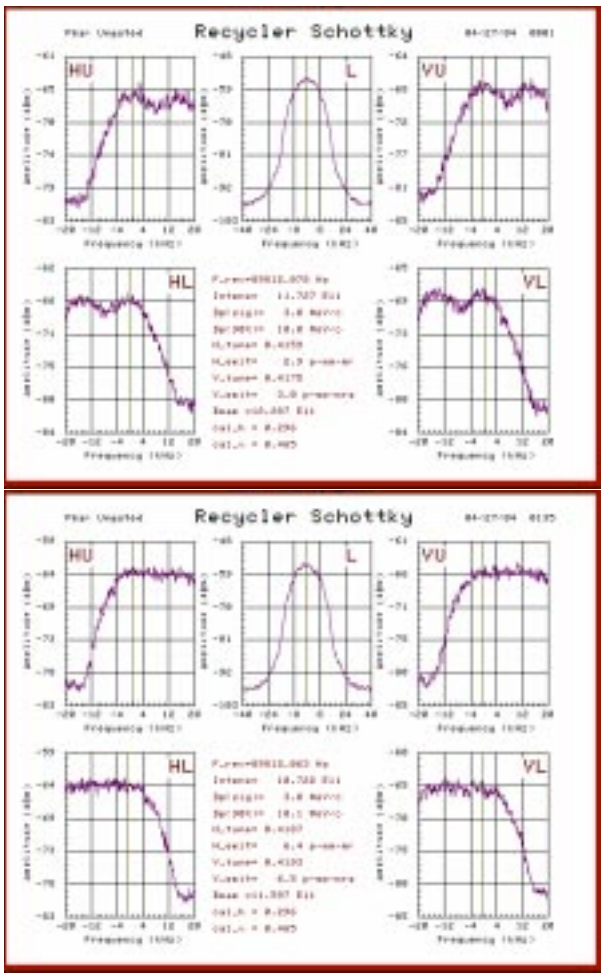

Figure 4: The betatron sidebands of the beam recorded by the 1.75 GHz Schottky detector (the two left plots and two right plots) are shown before (top) and after (bottom) the instability. The betatron sidebands were broadened during the instability while the longitudinal spread remained the same. (April 27 event)

To show the effect of the Main Injector ramp on the Recycler beam, we show in Fig. 5 the intensity of the Recycler beam overlayed on the ramp curves on the Main Injector starting from 01:00 for 40 minutes. The sharp narrow peaks are the Main Injector ramps, which occur roughly once very minute, but only two out of three are shown here.

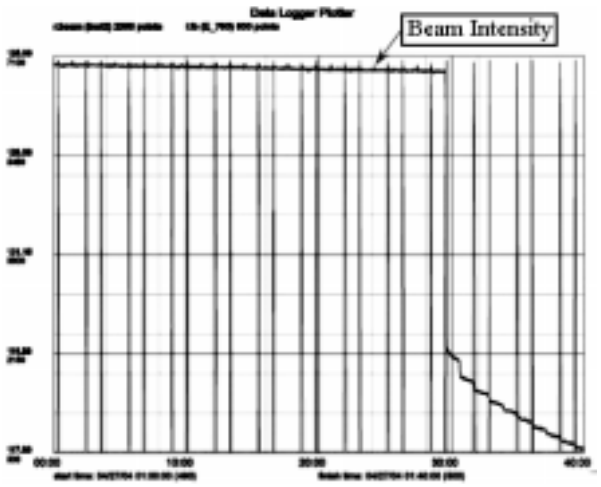

Figure 5: Main Injector ramps are plotted as a function of time, with only two of every three ramps shown. An antiproton beam of intensity 30×10^{10} was seen on March 8 to suffer a sudden beam loss right at the moment the Main Injector was ramped. Subsequent losses also occurred during later Main Injector ramps.

We can see clearly that the first beam loss occurred right at a ramp near 1:30 and subsequent smaller beam losses occurred whenever there was a ramp.

The most recent instability took place on June 4, where an antiproton beam of intensity 30×10^{10} and length 3.61 μs suddenly had its transverse emittances jumped from 3.4π mm-mr to 5.7π mm-mr with a beam loss of 0.5×10^{10}. At the same time, the rms momentum spread jumped from 1.9 MeV/c to 2.1 MeV/c. Notice that before this instability, the beam had been cooled to a much smaller rms momentum spread than the usual ~ 3 MeV/c.

Common Features

Some common features of these instabilities are:

1. The beams are all antiprotons of various lengths, from 5.28 μs to 9.3 μs, bunched in a barrier bucket.

2. The instabilities occurred with beam intensities either about 30×10^{10} or 125×10^{10}.

3. The transverse 95% normalized emittances of the beam have been cooled to less than 4π mm-mr, except for the February 19 event.

4. Every instability appears to be preceded at least one hour or more by a reduction in the ramp cycle of the Main Injector. The stray fields of the Main Injector during ramping affect the orbit of the Recycler Ring. Although there is a correction mechanism using beam-position monitors and bump magnets, the compensation has never been complete, especially when the ramp rate of the Main Injector is changed. The closed orbit of the Recycler beam will be pushed inwards and outwards according to the pulsation of the partially compensated stray fields.

Possible Mechanism

The above facts lead to the following possible mechanism for the instability:

1. The antiproton beam traps ions, since it becomes very unstable whenever the voltages of the clearing electrodes are turned off.

2. The ramping of the Main Injector situated underneath the Recycler Ring produces stray fields which heat the antiproton beam. The strength of the stochastic cooling has been adjusted to counteract this heating.

3. When the Main Injector lowers its ramping rate, there is less heating and the antiproton beam will be overcooled transversely.

4. The density of antiprotons increases and the beam traps more ions, resulting eventually in a transverse instability.

Although the above suggestion sounds rather appealing, verification has not yet been made. In addition, the fact that such instability has occurred only in antiproton beams but never in proton beams does not necessarily lead to the conclusion of trapped ions. This is because the Recycler Ring is designed to store and cool antiprotons but not protons. The pickups and kickers have been so arranged that the proton beam traveling in the reverse direction will see them in the wrong relative phase advances. For this reason, although antiprotons can be cooled to emittances 3π mm-mr or below, proton beams cannot be cooled at all. The smallest proton beam emittance is about 10π mm-mr. In other words, the proton beams have never been as dense as the antiproton beams transversely.

III. INDUCED INSTABILITIES

Since the above instabilities do not occur very often, to study them, we try to induce similar instabilities, although it is unclear whether what we induce are the same instabilities we observed before.

On March 5, an antiproton beam of intensity 19.7×10^{10} and length 9.3 μs in a barrier bucket was cooled to 95% normalized transverse emittances 2.5π mm-mr. The cooling was turned off and we see the emittances grow slowly in Fig. 6. About 17 min later, the barrier rf voltages were turned off. As the beam was fully debunched by filling the 1.83 μs gap, the emittances grew quickly to about 5.2π mm-mr. When the rf voltages were turned on again and cooling was resumed at 25 min, the emittances were damped. There is a sudden jump of the emittances similar to those observed in the previous instabilities.

A similar experiment shown in Fig. 7 was performed on March 9. The 9.3 μs antiproton beam of intensity 23.3×10^{10} was first cooled to 4.7π mm-mr. At 1800 s, cooling was turned off and the barrier voltages were reduced to zero. We see the transverse emittances rise rapidly. There was a sudden jump of the horizontal emittance but not for

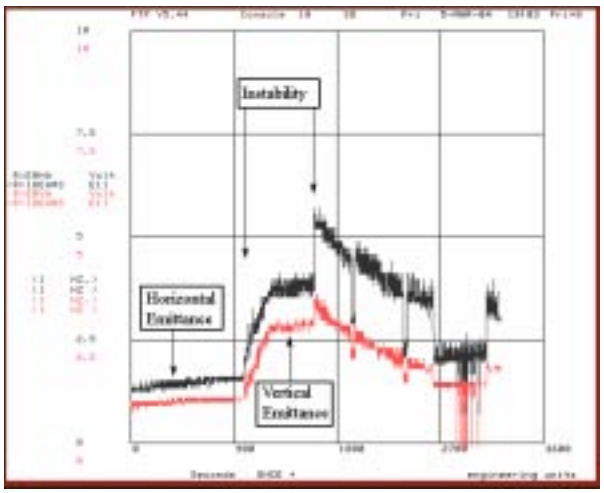

Figure 6: The horizontal and vertical 95% normalized emittances of a 9-μs antiproton beam in a barrier bucket are shown as functions of time. The emittances grew slowly when stochastic cooling was turned off at zero time. They grew rapidly when the rf was turned off at 17 min. The emittances were damped again when rf and cooling were resumed at 25 min. (March 5 experiment)

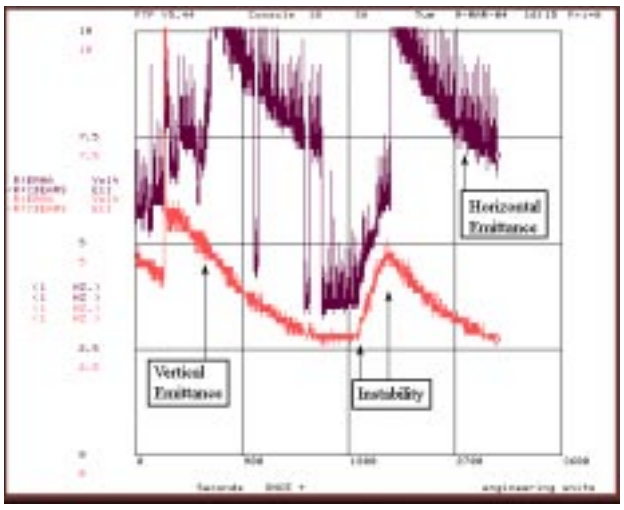

Figure 7: The horizontal and vertical 95% normalized emittances of a 9-μs antiproton beam of intensity 23.3×10^{10} in a barrier bucket are shown as functions of time. The emittances grew when stochastic cooling was turned off and the rf voltages reduced to zero at 1800 s. However, no coherent betatron sidebands were recorded successfully. (March 9 experiment)

the vertical. An attempt to measure coherent betatron sidebands had not been successful.

Another attempt was made on March 14 with a 78×10^{10} antiproton beam of length 9.3 μs inside a barrier bucket. The barrier voltage was reduced from 2 kV down to about 20 V. The gap started to fill with antiprotons and the instability was induced with transverse emittances blowup. The spectrum analyzer set to infinite persistence mode revealed betatron sidebands (Fig. 8) near the first four revolution harmonics, which ordinarily do not appear. No beam

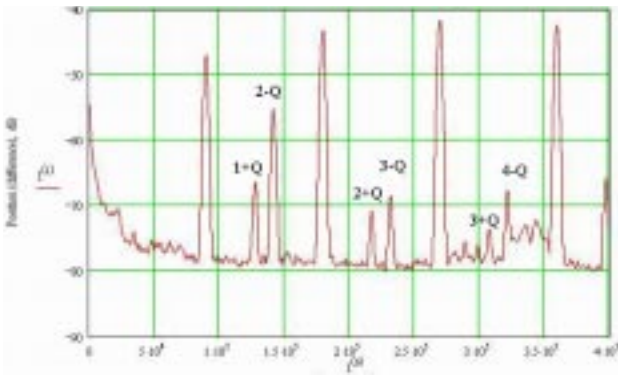

Figure 8: The transverse spectrum of a 9.3-μs antiproton beam of intensity 78×10^{10} was monitored up to 4 revolution harmonics with horizontal scale in Hz. When an instability was induced by reducing the barrier voltages from 2 kV to 20 V, coherent betatron sidebands were recorded. The larger unmarked peaks were the revolution harmonics. (May 14 experiment)

loss was recorded. The vertical small-amplitude angular bounce frequency of an ion with molecular weight A inside a antiproton beam of linear intensity $\lambda_{\bar{p}}$ and rms horizontal and vertical radii σ_h and σ_v is

$$\omega_i = \sqrt{\frac{2\lambda_{\bar{p}} r_p c^2}{\sigma_v(\sigma_h+\sigma_v)A}}\ , \qquad (1)$$

where $r_p = 1.5347\times10^{18}$ m is the classical radius of antiproton. Since the beam is completely debunched, the linear density is $\lambda_{\bar{p}} = 2.35\times10^8$ m^{-1}. The difference signals were collected at a split-tube vertical beam-position monitor at location VP522, where the horizontal and vertical betatron functions are, respectively, 47.6 m and 16.7 m. At the normalized transverse emittances of 6π mm-mr, the rms vertical and horizontal beam radii there were, respectively, 3.25 and 5.44 mm. The ions were mostly[2] CO^+ with $A = 28$. Thus the vertical ion bounce frequency was $\omega_i/(2\pi) = 45.4$ kHz, which is close to the $1-Q$ betatron sideband. Unfortunately, the amplifier driving the analyzer had poor response below the revolution frequency (89.81 kHz), which might explain why the $1-Q$ sideband had not been observed. The strongest betatron sideband in the spectrum is $2-Q$, corresponding to 142 kHz, which is close to the 170-kHz small-amplitude ion bounce frequency if the ion is H_2^+. It appears that the sidebands start to roll off after the second revolution harmonic.

The induced-instability experiments reported so far have nothing to do with the change in ramping pattern of the Main Injector. The two quadrupole buses of the Main Injector leave a net current of ~ 100 A around the circumference of the ring. The dipole field created by this difference current is usually compensated by passing an equal

[2] Although the residual gas in the vacuum chamber is compose of mostly hydrogen gas, however, the ionization cross section is 0.20 Mbarns, a factor of ten less than that for CO. For this reason, there are more CO^+ ions than H_2^+ ions.

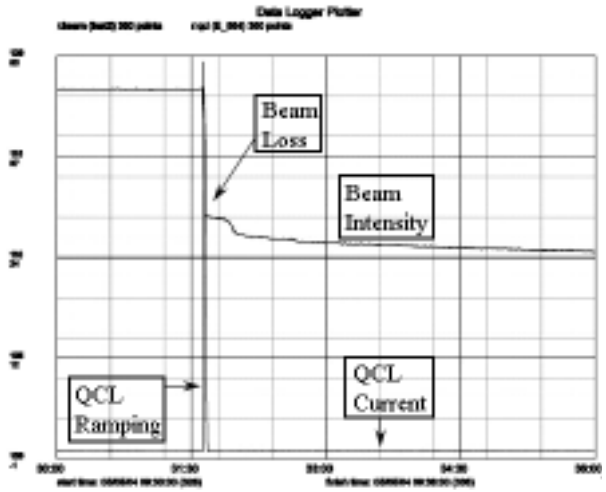

Figure 9: The intensity of a 5.3-μs antiproton beam is shown as a function of time. The intensity dropped suddenly from 117×10^{10} losing $\sim 6\times10^{10}$ right at the moment the quadrupole-correction loop (QCL) was pulsed. (May 5 experiment)

and opposite current through a quadrupole-correction loop (QCL) around the ring. Therefore pulsing the QCL will produce effects of the stray fields similar to a Main Injection ramp. On May 5, an experiment was performed to mimic the effect of the ramp pattern of the Main Injector on the Recycler instability using the QCL. One to two hours after the Main Injector stopped ramping, a Recycler beam of intensity 117×10^{10} of length 5.3 μ was prepared between two barriers. When the transverse 95% normalized emittances were cooled to 3π mm-mr, the QCL was pulsed for about 2 to 3 s. As shown in Fig. 9, the beam lost the intensity of 6×10^{10} right at the time the loop was pulsed. The transverse 95% normalized emittances jumped to 6π mm-mr as shown in Fig. 10. The transverse spectrum of the beam was also monitored by the same analyzer as before at VP522 up to the 4 revolution harmonics. The only difference is that the amplifier had been modified to have a flat response in the bandwidth from 10 kHz to 4 MHz. Unlike the results in Fig. 8, the analyzer recorded in Fig. 11 all the betatron sidebands up to 360 kHz. The small-amplitude ion bounce frequency at the moment before the emittance blowup is, according to Eq. (1), 114 kHz for CO^+, which is just slightly above the first revolution harmonics. As for H_2^+, the small-amplitude bounce frequency is 426 KHz, which is near the $5-Q$ sideband and is outside the scope of this measurement. Since we do not see any sign for the sideband power to roll off. The conclusion is either there is a large accumulation of H_2^+ or these sidebands and the transverse instability itself may not come from trapped ions. The betatron sidebands recorded by the 1.75-GHz Schottky detector before and after the instability are shown in the top and bottom plots of Fig. 12. The sideband Schottky signals are broadened after the instability and are very similar to those recorded in the observed instability on April 27 in Fig. 12.

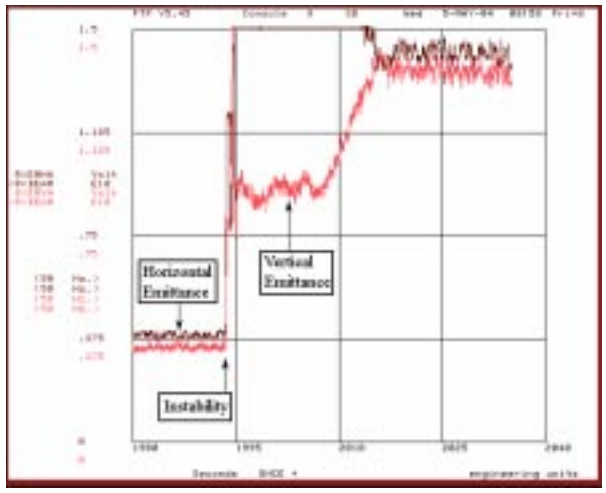

Figure 10: A 5.3-μs antiproton beam of intensity 117×10^{10} exhibits a jump in transverse emittances from about 3π mm-mr to more than 9π mm-mr. (May 5 experiment)

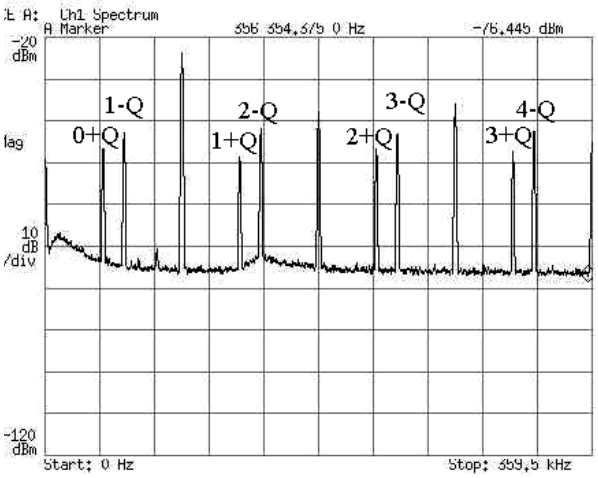

Figure 11: The analyzer shows betatron sidebands of harmonics from 0 Hz up to 359.5 kHz without any tendency of rolling off at higher frequencies. The noise floor peaks at 10 kHz and 143 kHz are there without beam. (May 5 experiment)

IV. ANALYSIS

Beam Gap

Assuming that an ion oscillates inside the antiproton beam and drifts in the beam gap, the transport matrix of the ion can be written easily. The half-trace of the transport matrix for one revolution turn is given by

$$\text{Half Trace} = \cos\phi_b - \frac{\phi_g}{2}\sin\phi_b\,. \qquad (2)$$

Denoting ω_i as the angular bounce frequency of the ion in the beam as expressed in Eq. (1), $\phi_b = \omega_i t_b$ is the transverse oscillation phase advance of the ion passing through

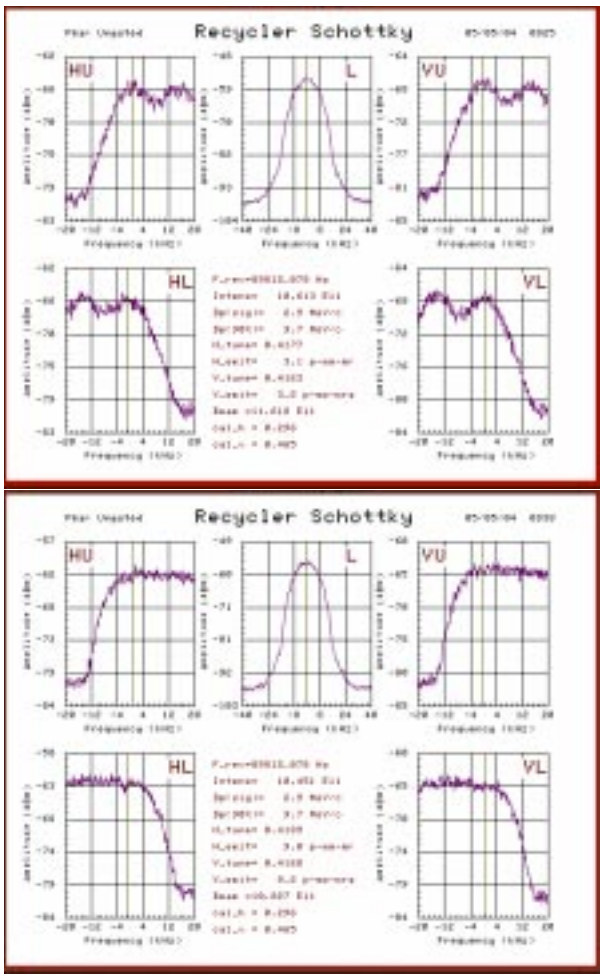

Figure 12: The betatron sidebands recorded by the 1.75-GHz Schottky detector (two left and two right plots) are shown before (top) and after (bottom) the instability. The betatron sidebands were broadened during the instability. (May 5 experiment)

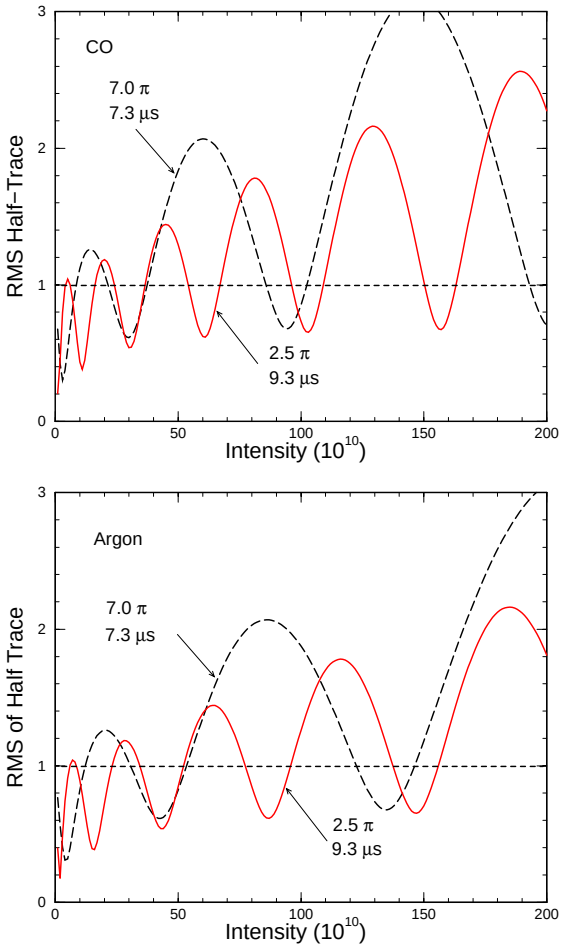

Figure 13: Plot of rms half-trace versus beam intensity for bunching length for the beam conditions of the February 19 and March 8 instabilities are shown in the top plot for CO^+ and the bottom plot for Ar^+. The plots show that at least one species of ions will not be trapped in the two situations.

the beam of length t_b, and $\phi_g = \omega_t(T_0 - t_b)$ is the phase advance of the ion with angular frequency ω_i in the duration of the passage of the beam gap of length $T_0 - t_b$. When the half-trace falls between ± 1, the ion is trapped, otherwise it will be cleared at the gap. [1] As a function of the beam intensity, the half-trace is oscillatory and it appears to be more appropriate to address instead the rms half-trace

$$\Big[\text{Half Trace}\Big]_{\text{rms}} = \left(\cos^2\phi_b + \frac{\phi_g^2}{4}\sin^2\phi_b\right)^{1/2} . \qquad (3)$$

We have computed the rms half-traces for all the different situations of the antiproton beams before the instabilities, either observed or induced. For H_2^+, the oscillation of the rms half-trace is fast with large amplitudes, indicating that they are not trapped at all. We show in Fig. 13, the rms half-traces for the February 19 (7.3 μs and 7.0π mm-mr) and March 8 (9.3 μs and 2.5π mm-mr) observed instabilities. We see that for the February 19 instability at the intensity of 126×10^{10}, the antiproton beam will trap Ar^+ but not CO^+. However, for the March 8 instability at the intensity of 30×10^{10}, the antiproton beam will trap CO^+ but not Ar^+. On the other hand, for the April 27 and June 4 instabilities, both Ar^+ and CO^+ will not be trapped. The results are summarized in Table 2 together with the beam conditions for the induced instabilities. What we obtain from the table are results contradicting observation. For example, all the antiproton beams before the induced instabilities can trap one species of ion and therefore should be unstable to begin with. On the other hand, the antiproton beams in the April 27 and June 4 observed instabilities cannot trap ions and therefore should be stable. However, one must remember that this linear model has been too simple to explain reality. First, it does not take into account of nonlinear elements in the ring. Second, it does not take into account the aperture of the ring. In other words, although ions may be trapped, they may oscillate with transverse amplitudes so large that they are eventually scraped by the vacuum chamber. Third, the ion bounce frequency ω_i used in the analysis has been the bounce frequency at small oscillation amplitudes. Most ions oscillating at larger amplitudes will

Table 2: The properties of the antiproton beams in the observed and induced instabilities are analyzed in the linear transport model to determine whether CO^+ or Ar^+ ions will be trapped (T) or untrapped (U).

Date	Bunch length (μs)	Emittance (mm-mr)	Intensity (10^{10})	Trapped or not CO^+	Ar^+
Observed instabilities					
Feb 19	7.3	7.0π	126	U	T
Mar 8	9.3	2.5π	30	T	U
Apr 27	5.3	3.0π	125	U	U
June 4	3.6	3.4π	30	U	U
Induced instabilities					
Mar 5	9.3	2.5π	20	U	T
Mar 9	9.3	4.7π	23	T	T
Mar 14	9.3	6.0π	78	T	U
May 5	5.3	3.0π	117	T	U

have much smaller bounce frequencies. The rms half-trace computed using the smaller bounce frequencies can lead to totally different trapped/untrapped results. As a result, not much can be concluded from this simple analysis. However, we may say that the occurrence of the observed instabilities and induced instabilities does not appear to have any relation to the length of the beam gap or whether the beam gap can clear the ions or not.

Coupled Beam-Ion Oscillation

While ions oscillate inside the antiproton beam, antiprotons will also oscillate about the ions. This coupled beam-ion oscillation theory was first proposed by Schnell and Zotter [2]. In the equation of motion for an antiproton, besides the external betatron focusing force, there is an additional focusing force from the ions. Thus, for the linearized restoring force, we can make the replacement

$$\omega_\beta^2 \longrightarrow \omega_\beta^2 + \omega_{\bar{p}}^2 \,, \tag{4}$$

where $\omega_\beta = \nu_\beta \omega_0$ is the betatron angular frequency in the absence of ions, and

$$\omega_{\bar{p}} = \sqrt{\frac{4\lambda_i r_p c^2}{\gamma\sigma_v(\sigma_v+\sigma_h)}} \,, \tag{5}$$

is the small-amplitude angular bounce frequency of the antiproton in ions in the absence of external betatron focusing, λ_i is the ion linear density, and σ_h and σ_v are the rms horizontal and vertical radii of the antiproton beam. Compared with the ion bounce frequency in Eq. (1), there is an extra relativistic factor of γ in the denominator because the beam particles are moving. There is an extra factor of 2 in the numerator because the ion beam has radii that are a factor of $\sqrt{2}$ smaller than those of the antiproton beam that generates them. The smaller ion beam radii arise from the assumption that the ions are generated without any transverse velocities.

In the presence of a sizable amount of ions trapped inside the antiproton beam, the ion bounce frequency in Eq. (1) should be replaced by

$$\omega_i = \sqrt{\frac{2\lambda_{\bar{p}}(1-\eta)r_p c^2}{\sigma_v(\sigma_h+\sigma_v)A}} \,, \tag{6}$$

since the charges of the antiprotons are partially shielded by the ions. Here, η is called the *neutralization factor*, defined as $\lambda_i = \eta\lambda_{\bar{p}}$. We therefore have

$$\omega_{\bar{p}}^2 = \omega_i^2 \frac{2A\eta}{\gamma(1-\eta)} \,. \tag{7}$$

Assuming that the beam fills the whole ring, the coupled-eigenfrequency of oscillation is solved in the usual way. An instability occurs when this eigenfrequency becomes complex, which is equivalent to

$$Q_{\bar{p}} > \frac{\left|(n-Q_i)^2 - \nu_\beta^2\right|}{\sqrt{4Q_i|n-Q_i|}} \,, \tag{8}$$

where $Q_i = \omega_i/\omega_0$ is the *ion-in-beam tune* and $Q_{\bar{p}} = \omega_{\bar{p}}/\omega_0$ is the *antiproton-in-ion tune* in the absence of external betatron focusing. For CO^+ in the March 5 experiment, the ion bounce frequency is $\omega_i/(2\pi) = 38.9$ kHz or $Q_I = 0.433$. With the vertical betatron tune $\nu_\beta = 24.415$, to make $|(n-Q_i)^2+\nu_\beta^2|$ as small as possible, we choose $n=-24$. Then the coupled beam-ion oscillation becomes unstable when $Q_{\bar{p}} > 0.137$, or neutralization $\eta > 0.0168$, which is very small. Once above threshold, the growth rate is given by

$$\frac{1}{\tau} \approx \frac{Q_{\bar{p}}\omega_0}{2}\sqrt{\frac{Q_i}{|n-Q_i|}} = 0.0092\omega_0 \,. \tag{9}$$

The actual growth rate will be much smaller because of the damping provided by the spread of the ion bounce frequency. The instabilities on March 5 and 9 were induced by turning off the barrier voltages so that the beam filled the whole ring. Very likely, they belong to this type of coupled beam-ion instability.

Fast-Ion Instability

Since the instabilities may not depend on the length of the beam gap, they may belong to the one-pass *fast-ion instability* proposed by Raubenheimer and Zimmermann. [3] Here, we assume that the beam gap is able to clear all the ions. Thus the ions experienced by the beam are accumulated from those generated from the head of the beam to the point of observation. Thus the tail of the beam will be seeing the largest ion linear density and will be seeing the same ion linear density all the time. This largest ion density is given by

$$\lambda_i = \Sigma n_g N_{\bar{p}} \,, \tag{10}$$

where $N_{\bar{p}}$ is the number of antiprotons in the beam, n_g is the residual gas density, and Σ is the cross section of producing an ion. At a vacuum pressure of 10^{-10} T, $n_g = 3.22\times10^{12}$ m^{-3} at room temperature. The ionization

cross section of CO^+ is about 2 Mbarn. Thus the largest ion linear density is $\lambda_i = 818$ m^{-1} at an antiproton intensity of $N_{\bar{p}} = 127\times10^{10}$, and this is very small compared with the linear density of the antiproton beam $\lambda_{\bar{p}} = 4.58\times10^{10}$ m^{-1} when the length of the beam is $t_b = 9.3$ μs. Obviously, the growth rate of coupled ion-beam oscillation will be very slow. An estimate of the non-*e*-folding growth time has been given by Chao and Stupakov, [4] where a uniformly transverse distributed particle beam with horizontal and vertical radii, a_h and a_v, is assumed. For this transverse distribution, the ion bounce angular frequency ω_i and the beam-in-ion bounce angular frequency $\omega_{\bar{p}}$ in the absence of external betatron focusing can be obtained from Eqs. (1) and (5) by replacing $\sigma_{h,v}$ by $a_{h,v}/\sqrt{2}$. The non-*e*-folding growth time in the linear theory can then be expressed as

$$\tau = \frac{2\omega_\beta}{\omega_{\bar{p}}^2\omega_i t_b} \ . \tag{11}$$

At the normalized 95% transverse emittances 6π mm-mr, antiproton beam intensity 127×10^{10}, and length of beam 9.3 μs, the growth time is $\tau = 12$ s when the vacuum pressure is 1×10^{-10} Torr. If the antiproton beam is cooled to the emittances of 3π mm-mr, the growth time becomes $\tau = 4.2$ s. In above, the full beam radii in the uniform distribution have been taken as $a_{h,v} = 2\sigma_{h,v}$ and the average horizontal and vertical betatron functions have been assumed to be $R/\nu_\beta = 21$ m, where R is the main radius of the Recycler Ring. The growth time will be further lengthened as a result of possible damping supplied by ion tune spread, betatron tune spreads, large-amplitude transverse oscillations, and stochastic cooling. The growth time in Eq. (11) can be rewritten as

$$\tau = \left[\frac{\gamma\beta^{1/2}\omega_\beta}{(2r_p)^{3/2}c^{5/2}}\right]\left[\frac{A^{1/2}}{\Sigma n_g}\right]\left[\frac{a^3}{N_{\bar{p}}^{3/2}t_b^{1/2}}\right] \ , \tag{12}$$

where we have assumed $a = a_h = a_v$. The first bracketed factor reflects the properties of the ring while the second bracketed factor reflects the ions and the third factor reflects the antiproton beam. For the beam, the most sensitive parameter is the transverse size. Thus the growth time decreases quickly if cooling is continued. For the ions, its residual density n_g is directly proportional to the vacuum pressure. Although the vacuum pressure of most the Recycler Ring is at 1×10^{-10} Torr, however, there is still a small unbaked region at 1×10^{-8} Torr. Ions trapped there will have a growth time 100 times smaller, or $\tau = 42$ ms when the emittances are 3π mm-mr.

If fast-ion instability is the mechanism, the growth in oscillation amplitude should increase along the antiproton beam. Thus one method of verification is to ping the head of the beam and measure the amplitude of oscillation along the beam by gating.

Half-Integer Stopband

Balbekov [5] pointed out that, because of the accumulated trapped ions, the observed instabilities might have been caused by the shifting of the antiproton betatron tunes into the half-integer stopbands. His theory is explained below. The incoherent vertical space-charge tune shift of a beam particle inside the antiproton beam is

$$\Delta\nu_{sc} = -\frac{N_{\bar{p}}r_p R}{\pi\gamma^3\beta^2 a_v(a_v+a_h)\nu_\beta} \ , \tag{13}$$

where R is the main radius of the ring, a_v and a_h are the vertical and horizontal beam radii, and uniform transverse distribution has been assumed. The factor $1/\gamma^2$ can be written as

$$\frac{1}{\gamma^2} = 1-\beta^2 \ , \tag{14}$$

where the "1" on the right side represents the electric contribution and the β^2 represents the magnetic contribution. When ions are trapped inside the antiproton beam, they cancel the charges of the antiprotons to a certain extent and an antiproton will be seeing a smaller electric force. With η denoting the fraction of neutralization so that $\lambda_i = \eta\lambda_{\bar{p}}$ inside the beam, we have

$$1-\beta^2 \longrightarrow 1-\eta-\beta^2 \ , \tag{15}$$

and the incoherent space-charge tune shift becomes

$$\Delta\nu_{sc} = \Delta\nu_{sc0}(1-\eta\gamma^2) \ , \tag{16}$$

where $\Delta\nu_{sc0}$ is the incoherent space-charge tune shift without any trapped ions. Thus when η is large enough, the magnetic contribution dominates over the electric contribution and $\Delta\nu_{sc}$ becomes positive. The horizontal and vertical betatron bare tunes of the Recycler Ring are, respectively, 25.425 and 25.415. With enough trapped ions, the betatron tunes may therefore be shifted into the half-integer stopbands resulting in a transverse instability.

A simple model is assumed with the antiproton beam of intensity $N_{\bar{p}}$ and length t_b having uniform transverse distribution. Assume that the ions of intensity $\eta N_{\bar{p}}T_0/t_b$ form a beam of the *same* transverse size as the antiprotons occupying all the circumference of the ring uniformly with uniform transverse distribution. For the sake of convenience, introduce a dimensionless reduced intensity

$$W = \sqrt{\frac{8\pi r_p R N_{\bar{p}}}{a_v(a_v+a_h)BA}} \ , \tag{17}$$

where $B = t_b/T_0$ is the bunching factor and $A = 28$ (40) is the molecular weight of the CO^+ (Ar^+) ion. Thus the ion bounce angular frequency is

$$\begin{cases} \omega_1 = \dfrac{W}{T_0}\sqrt{1-\eta} & \text{in beam } (0<t<t_b) \ , \\ \omega_2 = \dfrac{W}{T_0}\sqrt{\eta} & \text{in gap } (t_b<t<T_0) \ . \end{cases} \tag{18}$$

In the gap, an ion is actually expelled by the ion beam and performs hyperbolic motion. Therefore ω_2 should be addressed more properly as the exponential growth rate. The

half-trace of the transport matrix is

$$\text{Half-Trace} = \cos\phi_1 \cosh\phi_2 + \\ + \frac{1}{2}\left(\sqrt{\frac{\eta}{1-\eta}} - \sqrt{\frac{1-\eta}{\eta}}\right)\sin\phi_1 \sinh\phi_2 \,, \quad (19)$$

where $\phi_1 = \omega_1 t_b = WB\sqrt{1-\eta}$ is the betatron phase advance in the antiproton beam while $\phi_2 = \omega_2(T_0 - t_b) = W(1-B)\sqrt{\eta}$ is the hyperbolic growth decrement as the ion traverses the beam gap. Again, the ion will be trapped when the half-trace falls between ± 1. The half-trace is computed for an antiproton beam of bunching factor $B = 0.8$ but of different intensities. The results are plotted in Fig. 14. We

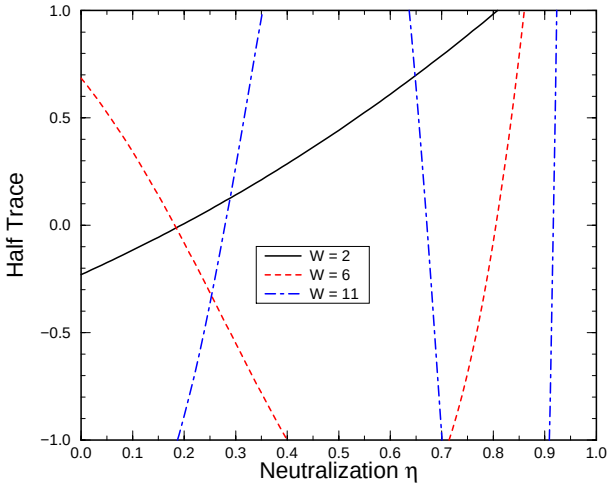

Figure 14: Plot depicting the half-trace of the transport matrix versus neutralization η at reduced intensity $W = 2$, 6, and 11, showing the corresponding maximum neutralization η arising from trapped ions.

see that at the reduced intensity $W = 2$, the $B = 0.8$ antiproton beam can continue to accumulate trapped ions until the neutralization $\eta \approx 0.8$, whereas at the reduced intensity $W = 6$, ions can be accumulated up to $\eta \approx 0.4$ only. On the other hand, at $W = 11$, no ions cannot be trapped at all. This maximum possible neutralization is plotted versus the reduced intensity W in Fig. 15 when the bunching factor is $B = 0.8$, 0.6, 0.4, and 0.2. It is clear that ions can be trapped at some reduced intensity W, but not for any W. For example, a $B = 0.8$ antiproton beam can trap ions up to neutralization $\eta \approx 0.8$ when reduced intensity is $W < 3.15$ and will not trap any when $3.15 < W < 3.95$. But when $3.95 < W < 6.40$, ion-trapping is again possible. We also see that when W is small, the maximum neutralization is roughly equal to the bunching factor ($\eta \sim B$).

The incoherent space-charge tune shift of Eq. (13) without trapped ions can be expressed in terms of the reduced intensity W via

$$\Delta\nu_{sc0} = -\frac{AW^2}{8\pi^2\nu_\beta\gamma^3} \,. \quad (20)$$

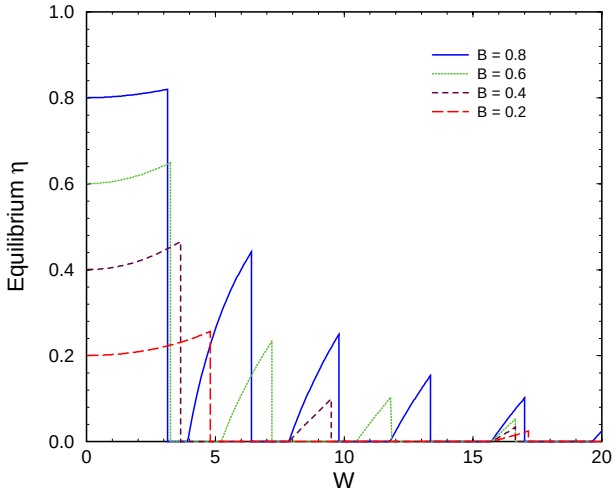

Figure 15: The maximum possible neutralization from trapped ions is shown as functions of the reduced beam intensity W for bunching factors $B = 0.8$, 0.6, 0.4, and 0.2.

The incoherent space-charge tune shift with neutralization $\Delta\nu_{sc}$ can now be plotted as functions of $\Delta\nu_{sc0}$ for both Ar^+ and CO^+. The plots of an antiproton beam with bunching factor $B = 0.8$ are shown in Fig. 16.

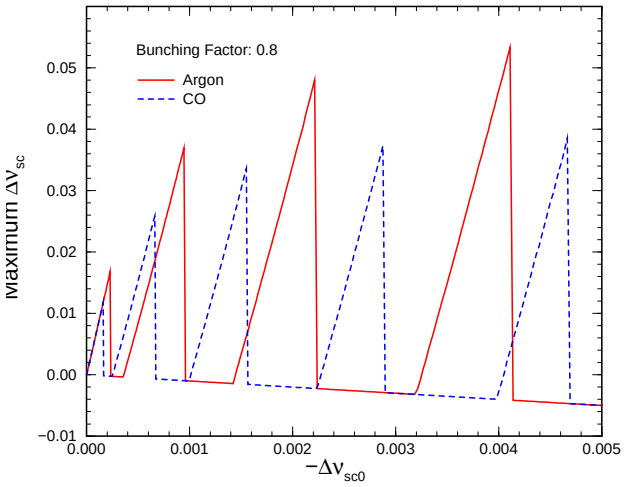

Figure 16: The incoherent space-charge tune shift of an antiproton beam with maximum allowable neutralization is shown as a function of the incoherent space-charge tune shift in the absence of ion trapping. The bunching factor is $B = 0.8$. Both CO^+ and Ar^+ ions are considered.

Every configuration of the antiproton beam corresponds to a $\Delta\nu_{sc0}$, the incoherent space-charge tune shift without trapped ions, and every $\Delta\nu_{sc0}$ corresponds to a maximum incoherent space-charge tune shift $\Delta\nu_{sc}$ neutralized by an ion species. We see in Fig. 16 that most values of $\Delta\nu_{sc0}$ will result in betatron tunes shifted upward towards the half-integer stopbands either due to the CO^+ ions or the Ar^+ ions. For example, consider an antiproton beam of intensity 100×10^{10} and bunching factor $B = 0.8$. At

the 95% normalized transverse emittances of $\varepsilon = 5\pi$ mm-mr, $\Delta\nu_{sc0} = -0.00066$ and $\Delta\nu_{sc}$ reaches 0.025 by trapping CO^+ ions. If the beam is cooled to $\varepsilon = 3.5\pi$ mm-mr, $\Delta\nu_{sc0} = -0.00093$, and $\Delta\nu_{sc}$ reaches 0.036 by trapping Ar^+ ions. When the beam continues to be cooled to $\varepsilon = 1.5\pi$ mm-mr, $\Delta\nu_{sc0} = -0.00219$, and $\Delta\nu_{sc}$ can be as large as 0.043 by trapping Ar^+ ions. Thus, it is quite possible that the betatron tunes will fall into the half-integer stopbands.

Comments

1. In this theory, the growth rate of the instability is not a monotonic function of the intensity of the antiproton beam or its transverse emittances. This is because an increase in beam intensity and/or a decrease of transverse emittances may sometimes move $\Delta\nu_{sc0}$ to a value that corresponds to a much smaller incoherent space-charge tune shift instead. In some sense, this effect resembles what we recorded in the observed instabilities and the induced instabilities.

2. One way to test this theory is to change the betatron tunes of the Recycler Ring. Knowing from Fig. 16 that the incoherent space-charge tune shift can be as large as $\Delta\nu_{sc} \approx 0.05$, if we decrease the betatron tunes of the Recycler Ring gradually by the amount 0.05, the transverse instabilities discussed in the paper will be avoided. However, we must be careful that the new betatron tunes will not be in the vicinity of the stopbands of other parametric resonances.

3. If this theory is correct, there should be large changes in the incoherent betatron tunes before and after an instability. Such changes, monitored by the 1.75 GHz Schottky detector, have so far been rather small and have not been large enough to hit the half-integer tunes. For this reason, the half-integer stopbands of the Recycler Ring should be computed to see whether they are unusually large.

V. CONCLUSION

We have reported the transverse instabilities observed recently in the Fermilab Recycler Ring. These instabilities have the signature of a sudden growth of the transverse emittances accompanied by a small beam loss. Instabilities of similar signature have been induced by reducing the rf voltages, turning off the cooling, and/or pulsing the quadrupole-correction loop to mimic a Main Injector ramp. The results of investigation indicate that the observed instabilities are closely related to the ramping pattern of the Main Injector and that trapped ions may play an important role. Some theoretical consideration has been presented. Although we suspect that the instabilities are related to ions trapped inside the antiproton beam, however, so far there has not been any direct proof of this conjecture.

REFERENCES

[1] D. Neuffer, E. Colton, D. Fitzgerald, T. Hardek, R. Hutson, R. Macek, M. Plum, and H. Thiessen, and T.-S. Wang, Nucl. Instr. Meth. A321 (1992) 1.

[2] W. Schnell and B. Zotter, CERN Report ISR-GS-RF/76-26, 1976.

[3] T.O. Raubenheimer and F. Zimmermann, Phys. Rev. E52 (1995) 5487.

[4] A.W. Chao and G.V. Stupakov, SLAC-PUB-7607, Proc. Int. Workshop on Multi-bunch Instabilities, Tsukuba, 1997.

[5] V. Balbekov, private communication.